

# Nickel plating by pulse electrolysis: textural and microstructural modifications due to adsorption/desorption phenomena

C. KOLLIA, N. SPYRELLIS

*Laboratory of General Chemistry, National Technical University of Athens, Zografou Campus, Athens 15773, Greece*

J. AMBLARD\*

*Laboratoire de Physicochimie des Rayonnements, Bâtiment 350, Centre d'Orsay, 91405 Cédex, France*

M. FROMENT, G. MAURIN

*Laboratoire de Physique des Liquides et Electrochimie, Université Pierre et Marie Curie, tour 22, 5e étage, 4 place Jussieu, 75252 Paris Cédex 05, France*

Received 28 November 1989; revised 21 February 1990

---

Nickel growth from an organic-free Watts bath working under d.c. plating conditions is governed by several interfacial inhibitors such as  $H_2$ ,  $H_{ads}$  or  $Ni(OH)_2$ . These inhibitors determine most of the structural or macroscopic properties of the nickel plates. Pulse electrolysis (p.e.) is thus a powerful means of perturbing the adsorption–desorption phenomena occurring at the nickel/electrolyte interface and hence offers an opportunity of preparing deposits exhibiting better properties. Through an analysis of the textural and microstructural changes produced by p.e., we show that molecular inhibitors desorb during the relaxation time, while conversely other inhibitors like  $H_{ads}$  or anions are more strongly adsorbed and inhibit the nickel cathodic process.

---

## 1. Introduction

Because of several specific advantages over conventional d.c. plating, p.e. is increasingly used as a routine technique to prepare metallic plates exhibiting better properties. This is especially true for diffusion-controlled electrochemical systems such as dilute solutions of noble metals [1–7], and also for the electro-deposition of various alloys [8–17].

Comparatively, pure nickel electrocrystallization under p.e. conditions has been much less studied, the major reason being that it is a slow cathodic process in which mass transport phenomena of  $Ni^{2+}$  ions are not expected to play a relevant role. Nevertheless, we have shown that p.e. could exert a strong influence upon the structural properties of nickel deposits, namely upon their preferred orientation or texture [18, 19], which gives an additional tool for elucidating the adsorption-desorption phenomena governing nickel growth at the cathode-solution interface.

The aim of the present work is twofold. Starting from several well-defined d.c. plating conditions, leading to given textures and thus to given properties, we first describe the structural modifications which are brought about by p.e. and hence the macroscopic

properties (e.g. brighter or smoother deposits) which can be expected from pulse plated deposits. Another more fundamental standpoint is to understand the same structural modifications in terms of perturbation of the cathodic process: if the same growth model we proposed for nickel electrocrystallization under d.c. conditions [20–26] still holds for p.e. plating, then the structural modifications may become predictable from the mere effect of p.e. upon the parameters governing nickel growth. We had shown previously that nickel electrocrystallization under d.c. steady-state conditions is governed by intrinsic interfacial inhibitors which are formed during the cathodic process as a consequence of hydrogen codeposition [20–22]. Hence p.e. is a means of perturbing the cathodic layer, so as to determine which interfacial inhibitor is adsorbed (or desorbed) during the plating ON-time  $T$  or during the relaxation OFF-time  $T'$ . The additional parameters  $T$  and  $T'$  can be chosen independently. This gives two more degrees of freedom regarding the choice of plating conditions. However, in order to be able to draw reliable conclusions, we have restricted the present study to only three different d.c. conditions (see Table 1 below) which are progressively perturbed by the pulse regime.

\*To whom correspondence should be sent.

Table 1. The d.c. plating parameters defining three reference states which will be submitted to a progressive p.e. perturbation. In every case the solution is a Watts bath at 50° C.

Cathodic potential V/SCE	-0.800	-0.96	-0.96
Peak current density $J_p$ , A · dm <sup>-2</sup>	1.5	25	25
Bulk pH	4.5	1.5	4.5
Texture axis or mode of growth	<211>	<210>	[100]
Kind of intrinsic interfacial inhibitor	Ni(OH) <sub>2</sub>	H <sub>2</sub>	

## 2. Experimental details

Plating parameters were kept rigorously the same as those described in our previous papers concerning d.c. plated nickel [20–22, 24]. They were chosen, as summarized in Table 1, so as to lead to nickel deposits exhibiting, in each case, the highest degree of texture perfection. The unique difference of the present study lies in the additional ability of monitoring the cathodic potential to be commutated periodically between  $V$  for a time  $T$  and  $V'$  for a time  $T'$ . This was achieved by means of a microprocessor-monitored potentiostat delivering square potentiostatic pulses.  $V$  was chosen so as to give the desired peak current density  $J_p$ ;  $V'$  was in every case  $-400$  mV/SCE, i.e. a potential under which no deposition occurs.  $V$  and  $J_p$  were kept constant for one set of experiments, while  $T$  and  $T'$  were varied independently over a broad range ( $10^{-5}$  s– $10^2$  s).

From the three parameters  $T$ ,  $T'$  and  $J_p$ , all the other pulse parameters commonly used were readily deduced:

- the pulse period  $\theta = T + T'$
- the pulse frequency  $\theta^{-1}$
- the duty cycle  $T \times \theta^{-1}$
- the average current density  $J_m = J_p \times \theta^{-1} \times T$

Once the deposits were sufficiently thick to be studied by X-ray diffractometry [20], a quantitative texture analysis was carried out. Then the deposits were submitted to electron microscopic investigations using either TEM or SEM techniques.

## 3. Results and discussion

Textural modifications provoked by p.e. are summarized in the diagrams given in Figs 1, 5 and 6, which are plots of pulse frequency against duty cycle. These diagrams show the existence of several domains wherein the nickel deposits exhibit the same preferred orientation axis  $[hkl]$ , i.e. the same mode of growth induced by a specific interfacial inhibitor [24]. To achieve better characterization of the perturbation provoked by the pulse regime, these raw texture results have to be completed with quantitative X-ray diffraction analysis, as well as with microstructural data given by electron microscopy.

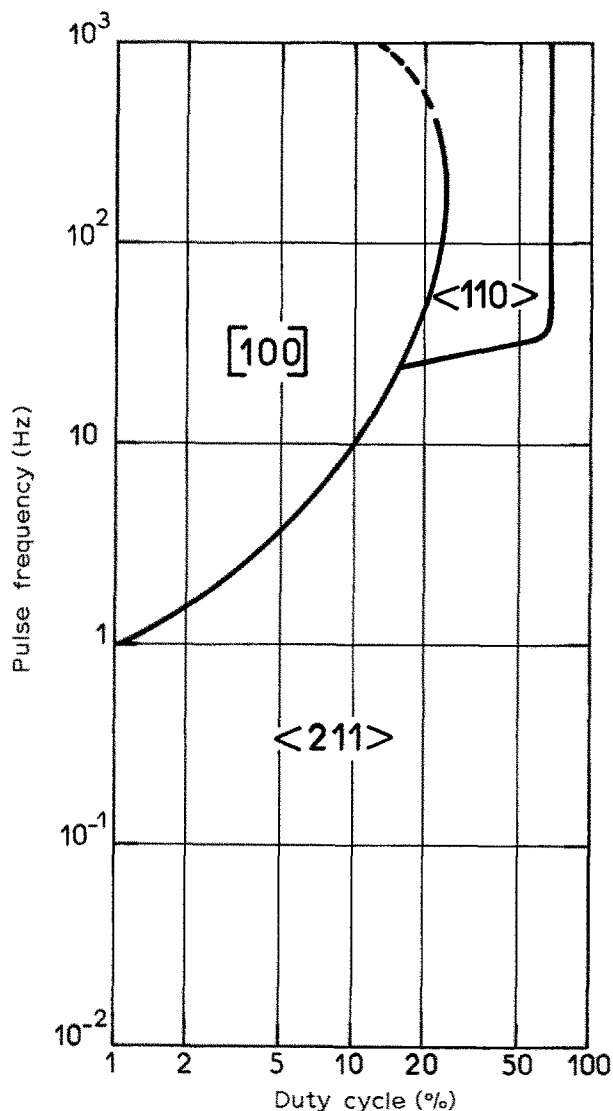


Fig. 1. Modification of a d.c. <211> texture under p.e. plating conditions.

### 3.1. Perturbation of the <211> mode of growth

Starting from the d.c. reference state, which corresponds to the vertical line on the right side of Fig. 1 (for a duty cycle = 100%), the perturbation of p.e. may be characterized either by shorter ON-times,  $T$ , (i.e. by low values of duty cycle) or by high pulse frequencies. It can be seen on the texture diagram that there exists a broad domain where <211> is preserved. This inhibited mode of growth is replaced by the freer mode [100] for a stronger perturbation, or even by <110> for higher pulse frequencies. As for the <211> → [100] transition, it can be readily explained in terms of the desorption (or the retrodiffusion towards the bulk solution), during the OFF-time, of the colloidal Ni(OH)<sub>2</sub> which was formed during  $T$ . We shall discuss below the case of the <211> → <110> transition which may be more difficult to understand.

What can be seen on Fig. 2 is the difference in the morphology along the same radius of the rotating disc cathode: both micrographs of Fig. 2 were taken from the same plate whose depositing conditions corre-



Fig. 2. TEM investigations of a deposit at the  $\langle 211 \rangle \rightarrow \langle 110 \rangle$  boundary (duty cycle 60%; pulse frequency 60 Hz). Scale bars: 1  $\mu\text{m}$ . (a) typical  $\langle 211 \rangle$  crystallite near the cathode edge; (b) finer grain sized  $\langle 110 \rangle$  crystallites at the centre of the disc cathode.

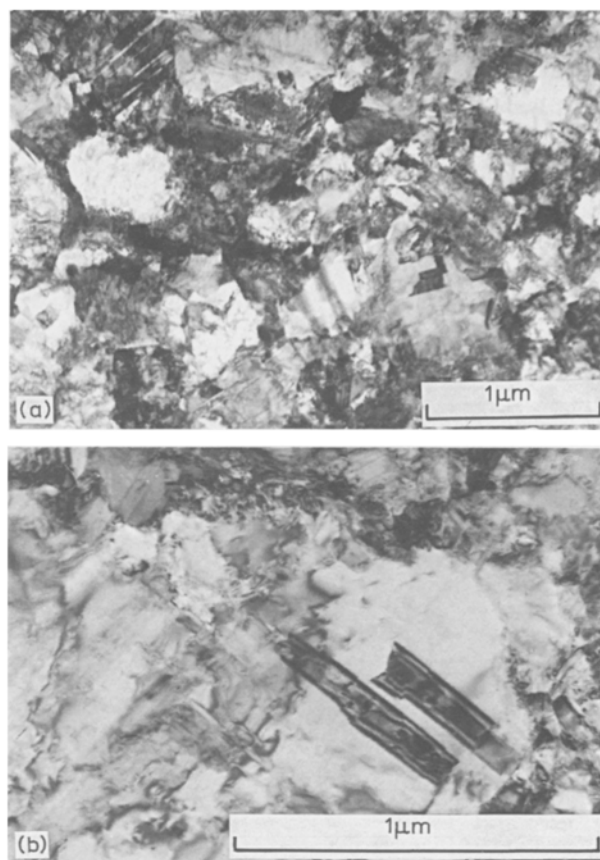


Fig. 3. TEM examination of a deposit near the  $\langle 110 \rangle \rightarrow [100]$  boundary (20% duty cycle;  $10^2$  Hz). Scale bars: 1  $\mu\text{m}$ . (a) typical  $[100]$  oriented small crystallites exhibiting numerous structural defects; (b) well developed  $[100]$  crystallite.

spond to the  $\langle 211 \rangle \rightarrow \langle 110 \rangle$  boundary (60% duty cycle; pulse frequency 60 Hz). Near the cathode edge the crystallites exhibit the typical morphology [27–29] of the  $\langle 211 \rangle$  preferred orientation (2a), while the center of the same deposit is made up of  $\langle 110 \rangle$  crystallites of finer grain size (2b).

Figure 3 shows two micrographs of a deposit plated under conditions close to the  $[100] \rightarrow \langle 110 \rangle$  boundary: 20% duty cycle;  $10^2$  Hz. The plate consists of small  $[100]$  grains containing numerous structural defects (3a). The largest well developed typical  $[100]$  crystallite has a size less than 1  $\mu\text{m}$  (3b), i.e. much less than a typical d.c.  $[100]$  crystallite [27].

Better developed  $\langle 110 \rangle$  crystallites can be found in the  $\langle 110 \rangle$  texture domain away from its boundaries. The deposit of Fig. 4a was grown under 60% duty cycle and  $10^2$  Hz: one can see a typical fivefold symmetrical  $\langle 110 \rangle$  crystallite exhibiting a remarkable preferential growth along its five vertical twin planes. Such a crystalline morphology strongly suggests a severe interfacial inhibition, which only permits the growth in the vicinity of what has been proved to be the most active growth sites [29]. The same kind of inhibition should be even more severe under a stronger p.e. perturbation. However, a nickel plate obtained under lower duty cycle (40%) and higher pulse frequency ( $10^3$  Hz) shows a crystalline morphology (Fig. 4b) resembling that of a  $\langle 110 \rangle$  deposit grown under d.c. conditions [30].

That somewhat puzzling result probably stems from the capacitance effects depicted by IBL [6]: beyond the limit where the ON-time is of the same order of magnitude as the charging time of the electrical double layer ( $\sim 5 \times 10^{-4}$  s in this case), the current modulation induced by the pulse regime is considerably damped.

### 3.2. Perturbation of the $\langle 210 \rangle$ mode of growth

The whole effect of p.e. upon the d.c.  $\langle 210 \rangle$  mode of growth is shown in the texture diagram of Fig. 5, which roughly presents the same features as in the case of  $\langle 211 \rangle$ : the d.c.  $\langle 210 \rangle$  texture is preserved (and ameliorated) at low pulse frequencies and high duty cycle values. It does exist, whatever the duty cycle and the average current density, at pulse frequencies less than 1 Hz.

For medium pulse frequencies (1 to  $10^2$  Hz) we observe the expected texture transition  $\langle 210 \rangle \rightarrow [100]$ . Such a transition, which had been previously observed [18, 19, 31], has to be related to the retrodiffusion of hydrogen away from the cathodic surface where it is formed abundantly under these plating conditions [20–22, 32, 33].

Under the most p.e. perturbed conditions, one observes the transition  $[100] \rightarrow \langle 110 \rangle$ . The  $\langle 110 \rangle$  mode of growth is only stable over a restricted area where pulse frequency is higher than 400 Hz and duty

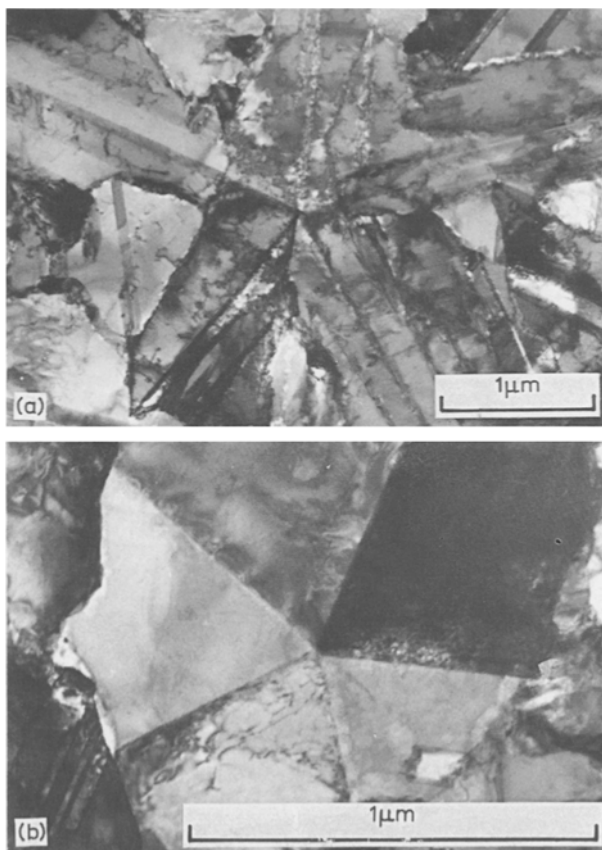


Fig. 4. Two different kinds of  $\langle 110 \rangle$  growth under strongly perturbed p.e. conditions. Scale bars:  $1 \mu\text{m}$ . (a) micrograph obtained from a (60% duty cycle;  $10^2$  Hz) deposit, showing a preferential growth along twin planes arranged in a fivefold symmetry; (b) micrograph of a (40% duty cycle;  $10^3$  Hz) deposit, showing a growth resembling that of a  $\langle 110 \rangle$  deposit plated under d.c. conditions.

cycle less than 10%, which means for the shortest ON-times  $T$ . Now it has been proved that very short ON-times favour the formation of a very thin pulsating diffusion layer [6].

This should not affect nickel deposition directly since the process is not controlled by diffusion. However, it may enhance the formation of adsorbed atomic hydrogen ( $H_{\text{ads}}$ ), a process which was shown to be diffusion-controlled on a nickel cathode [34]. Moreover, it must be stressed that the  $\langle 110 \rangle$  mode of growth has been ascribed to a selective inhibition of the nickel catholyte interface by  $H_{\text{ads}}$  [20–22]. There appears to be a contradictory effect exerted by pulse electrolysis: the  $\langle 210 \rangle \rightarrow [100]$  transition occurs because the cathodic interface is relieved from the adsorbed molecular hydrogen, while another kind of inhibition stems from a reinforced adsorption of atomic hydrogen which provokes the  $[100] \rightarrow \langle 110 \rangle$  transition. Note that both kinds of inhibition concern well separated areas of the texture diagram, otherwise the  $[100]$  free mode of growth would have been unnoticed.

### 3.3. Perturbation of the $[100]$ mode of growth

The above considerations are consistent with the texture diagram of Fig. 6 where no transition occurs,

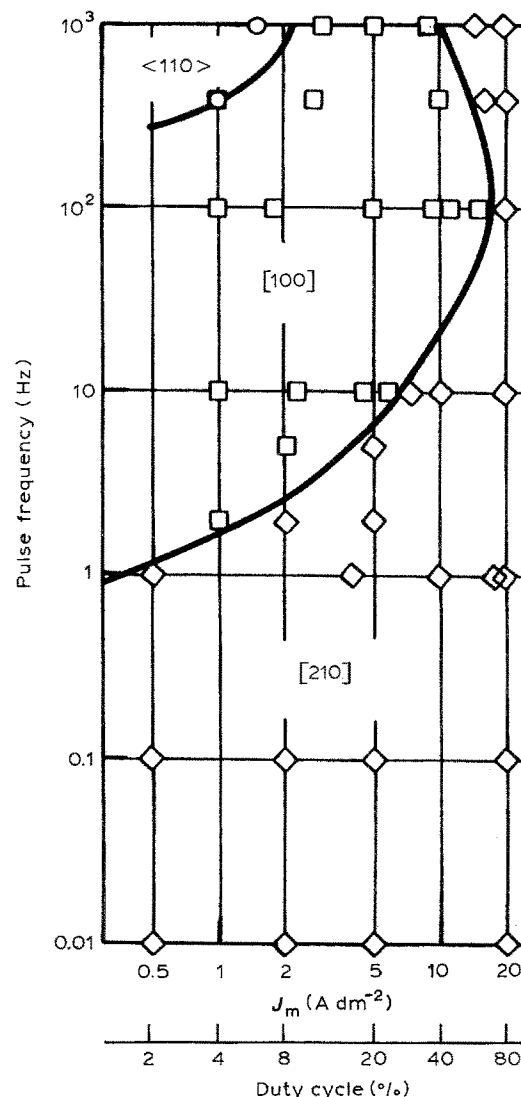


Fig. 5. Modification of a  $\langle 210 \rangle$  texture under p.e. plating conditions.

except the same  $[100] \rightarrow \langle 110 \rangle$  transition that was also observed in the diagrams of Fig. 1 and Fig. 5. That no other textures appear is also consistent with the growth model depicting the  $[100]$  preferred orientation as the free mode of growth for electrolytic nickel [20–24]. The preponderance of  $[100]$  in the whole diagram is an additional proof that no specific interfacial inhibitor is involved here. Moreover, the exceptional stability of  $[100]$  over a broad range of p.e. conditions gives an opportunity of examining more thoroughly the effect of p.e. upon texture and morphology.

Figure 7 allows a comparison between a d.c. reference deposit (7a) and a p.e. deposit (7b) obtained under very slight p.e. conditions: 95% duty cycle and  $10^{-2}$  Hz. Both micrographs show typical  $[100]$  grains, with an obviously better crystallization in the p.e. sample, i.e. larger grain size and much fewer structural defects. This means that the OFF-time gives the cathodic layer an opportunity for the desorption of interfacial inhibitors such as  $H_2$  or  $Ni(OH)_2$ . Although they do not play a major role, since here they are not abundant enough to provoke a texture transition (towards  $\langle 210 \rangle$  or  $\langle 211 \rangle$ , respectively), they do

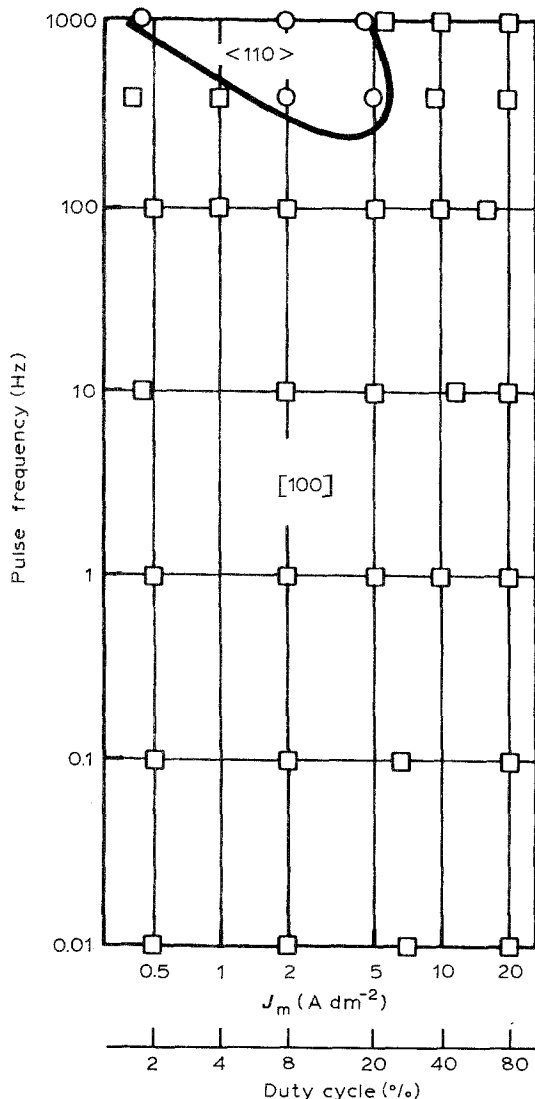


Fig. 6. Modification of a [100] texture under p.e. plating conditions.

exert a slight inhibiting effect which is evidenced by the small amount of random oriented crystallites that always exists in d.c. [100] deposits [20]. The random component readily disappears under slight p.e. conditions, i.e. low pulse frequencies ( $\leq 10$  Hz) and high duty cycles ( $\geq 80\%$ ). This gives a means of preparing deposits of higher purity, lower hardness and larger grain size, containing much fewer structural defects and foreign species.

Now the question is: Does a long OFF-time result systematically in better properties? Both plates of Fig. 8 were prepared at the same low pulse frequency ( $10^{-2}$  Hz), but with quite different duty cycles, 95% (8a) and 2% (8b) respectively. The latter shows a smaller grain size and a higher density of structural defects, while its textural perfection  $Q_{100}$  is ten times smaller. This means that a prolonged OFF-time is damaging, probably because of the poisoning of the growth sites due to an adsorption of anions (or other foreign species) from the bulk solution. Such a deactivation of the growth sites implies that a renucleation process has to take place in order to initiate the deposit during the next pulse.

What happens now under a strong p.e. perturbation?

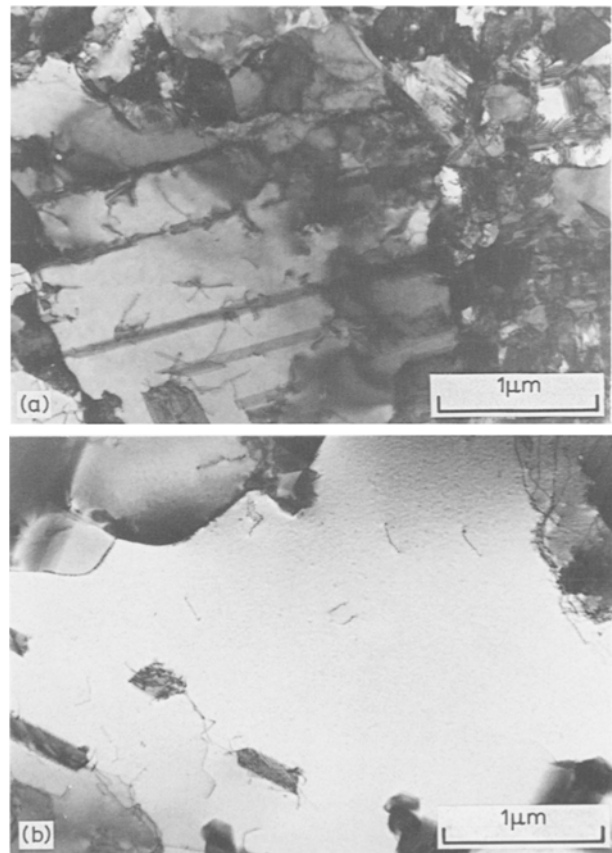


Fig. 7. TEM investigations showing the effect of a very slight p.e. perturbation upon the [100] mode of growth. Scale bars:  $1\mu\text{m}$ . (a) d.c. [100] deposit with a typical twinned [100] crystallite and disordered areas consisting of smaller grains; (b) p.e. [100] deposit (95% duty cycle;  $10^{-2}$  Hz) with larger grains and less structural defects.

The two micrographs of Fig. 9 allow a comparison between a d.c. plated (9a) and a p.e. deposit (9b) corresponding to a 20% duty cycle and a  $10^2$  Hz pulse frequency. The corresponding point on the texture diagram (Fig. 6) still lies in the [100] domain, though not very far from the [100]  $\rightarrow$   $\langle 110 \rangle$  boundary. What can be seen in Fig. 9b is a dramatic grain refinement, while the textural perfection is five times lower than in the d.c. case. Moreover, by measuring the pH increase during electrolysis in both cases, we found no variation in the d.c. case and a slight, although noticeable, increase in the p.e. case (0.03 pH unit). This result shows that a too strong p.e. perturbation enhances hydrogen adsorption, thus giving a nickel growth inhibition.

This tendency may become more evident with a pulse duration twice as short, as can be seen on the two micrographs of Fig. 10. The first (10a) is taken from the same p.e. deposit as shown in Fig. 9b, here depicted in a higher magnification. The second (10b) is a p.e. deposit prepared with the same pulse frequency, but with a 10% duty cycle. Many more structural defects are seen in the second case. That these defects result from an enhancement of hydrogen adsorption is confirmed by the definite pH increase measured here (0.14 pH unit).

Keeping in mind that the macroscopic properties of the plates are closely related to the structural data

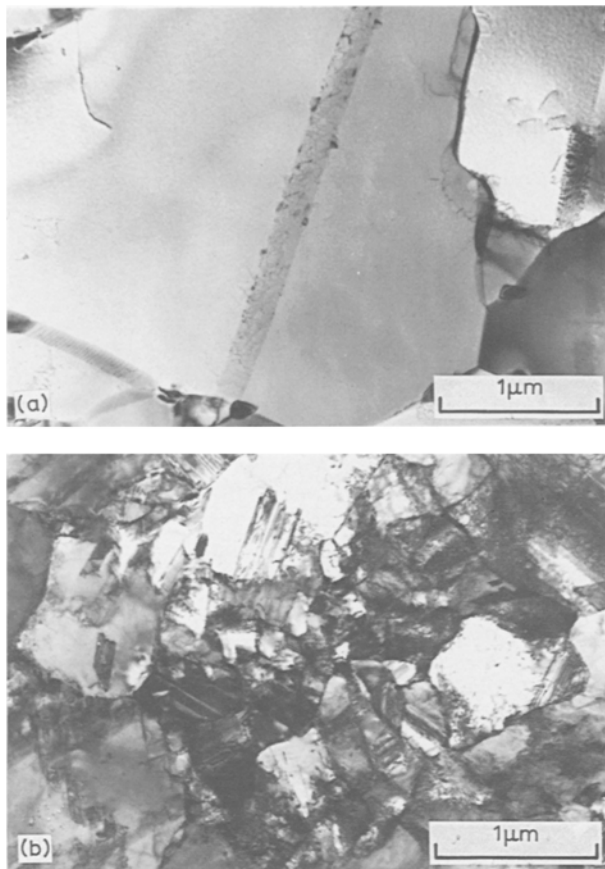


Fig. 8. TEM results showing the effect of the relaxation time upon the structure of p.e. [100] deposits obtained with the same pulse frequency ( $10^{-2}$  Hz). Scale bars:  $1\ \mu\text{m}$ . (a) 95% duty cycle; (b) 2% duty cycle.

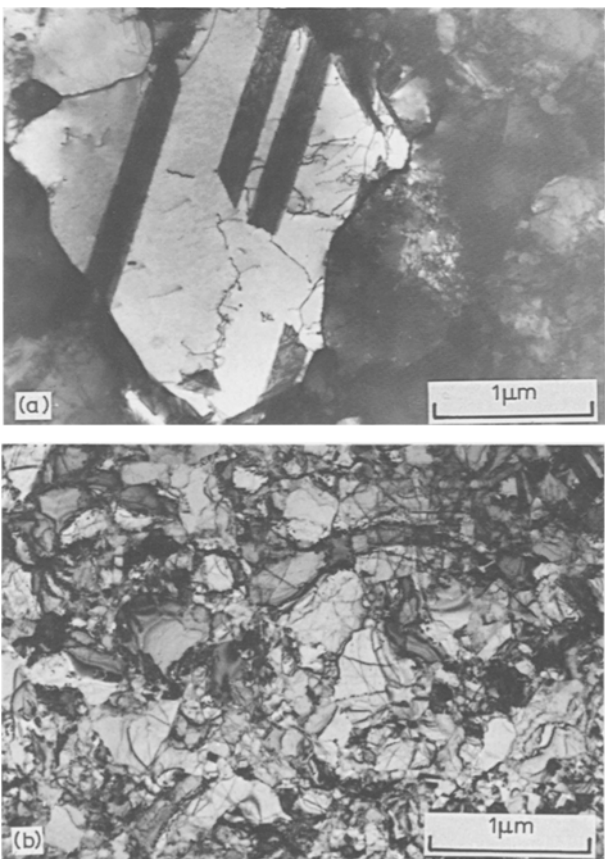


Fig. 9. TEM observation of a strong p.e. perturbation in [100] deposits. Scale bars:  $1\ \mu\text{m}$ . (a) d.c. reference deposit; (b) semibright p.e. deposit (20% duty cycle, pulse frequency  $10^2$  Hz).

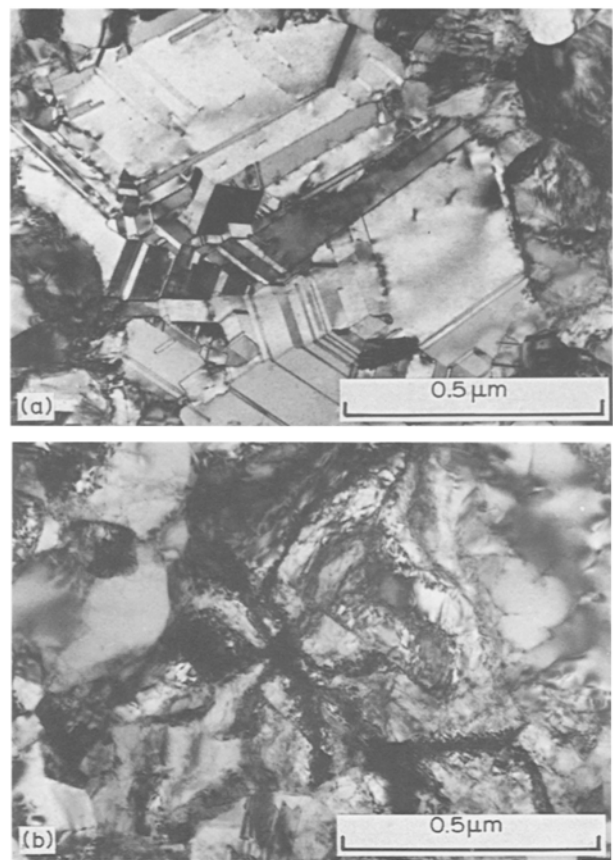


Fig. 10. TEM observation of two semibright [100] deposits plated under a strong p.e. perturbation. Scale bars:  $0.5\ \mu\text{m}$ . (a) 20% duty cycle and  $10^2$  Hz; (b) 10% duty cycle and same pulse frequency (brighter deposit).

given above, it is now possible to draw some conclusions about those properties which are of practical use, for example brightness. Brightness has been proved to be highly dependent on the surface morphology [29]: it is higher the lower the microrelief, i.e. the lower the grain size. By achieving grain refinement, as shown in Fig. 10, without making use of organic additives, p.e. appears to be a means for preparing semi-bright nickel plates.

All the results concerning [100] p.e. deposits show the dramatic effect of hydrogen codeposition in nickel electrocrystallization. Such an effect is, of course, the more drastic the nearer we approach the [100]  $\rightarrow$   $\langle 110 \rangle$  transition, beyond which it becomes conspicuous. However, it can be seen at a fair distance from the  $\langle 110 \rangle$  domain, even for a medium perturbation. We have plotted in Fig. 11 the profiles of the (400) Bragg reflections corresponding to a d.c. plate (11a) and to a p.e. plate (11b). The latter was prepared at 10 Hz with an 8% duty cycle. The evident broadening of the X-ray line registered with the p.e. deposit means that it is made of shorter fibres, which accounts for its semi-bright aspect, while the d.c. deposit looks dull.

#### 4. Conclusion

The rather complex perturbation of nickel growth provoked by p.e. is summarized in Fig. 12. Starting from the d.c. reference state, which is represented by the 100% duty cycle line, two arrows indicate which kind of

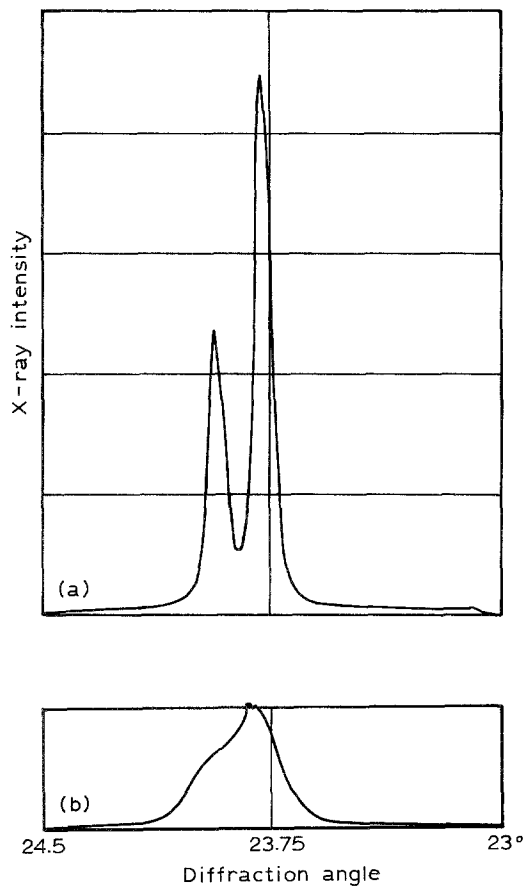


Fig. 11. Broadening of the (400) Bragg reflection due to the shortening of fibers induced by the p.e. perturbation. (a) d.c. reference [1 0 0] deposit. (b) p.e. [100] deposit plated under 8% duty cycle and 10 Hz pulse frequency (the texture perfection is only divided by a factor 2.3).

adsorption-desorption phenomena are likely through a given choice of plating conditions. The solid arrow indicates the direction towards the most perturbed plating conditions, which are encountered for the shortest pulse duration, i.e. the lowest duty cycle values and the highest pulse frequencies.

The p.e. perturbation finds its own limit when the ON-time is of the same order of magnitude as the time required for the electrical double layer to be charged. Then the p.e. perturbation results in a current modulation that increasingly resembles d.c. conditions. The use of p.e. should therefore be restricted to a pulse frequency of  $10^2$  Hz for  $\langle 211 \rangle$ , and  $10^3$  Hz for  $\langle 210 \rangle$  and [1 0 0] d.c. starting conditions.

Along the solid arrow three different cases have to be distinguished:

- very small perturbations result in better crystallized dull deposits with larger grain size and much fewer structural defects;
- medium perturbations allow the desorption of interfacial inhibitors such as  $H_2$  or  $Ni(OH)_2$ , but enhance the adsorption of atomic hydrogen;
- large perturbations lead in every case to the appearance of the  $\langle 110 \rangle$  mode of growth which suggests a severe growth inhibition brought about by  $H_{ads}$ .

Insofar as semi-bright deposits are sought for, a

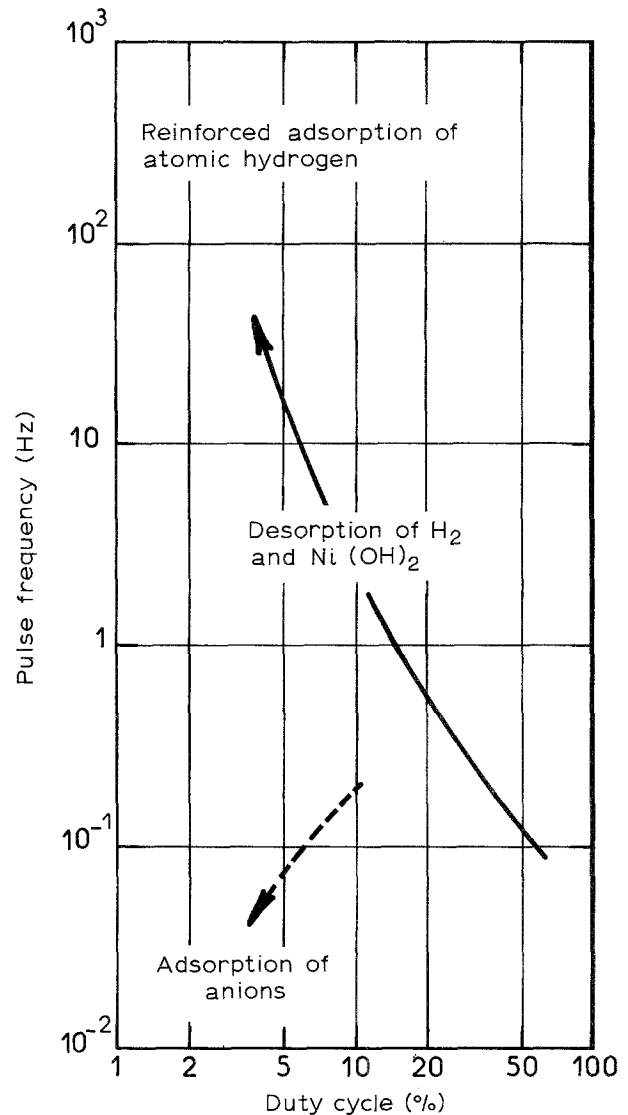


Fig. 12. Schematic representation of perturbations of nickel electrocrystallization due to pulse electrolysis. Following the solid arrow, we first meet a medium perturbed area where the cathodic layer is relieved from specific interfacial inhibitors such as molecular hydrogen or  $Ni(OH)_2$ , then a strongly perturbed area where every kind of texture turns to  $\langle 110 \rangle$ . An additional perturbation effect is evidenced (along the dotted arrow) for prolonged relaxation times, when anions or other poisoning species from the bulk are blocking the growth sites.

medium perturbation (e.g. 10 to  $10^2$  Hz; 10 to 20% duty cycle) has to be used.

Along the dotted arrow, another source of perturbation has also been demonstrated for prolonged relaxation times. This shows a reinforced adsorption process of anions from the bulk solution.

The results presented here show that the choice of proper p.e. plating conditions is far from clear, mainly because many intricate adsorption-desorption phenomena are involved.

References

[1] A. J. Avila and M. J. Brown, *Plating Surf. Finishing* 57 (1970) 1105.  
 [2] N. Ibl, J. C. Puipe and H. Angerer, *Surf. Techn.* 6 (1978) 287.  
 [3] J. C. Puipe, N. Ibl, H. Angerer and H. J. Schenk, *Oberfläche-Surface* 20 (1979) 77.

- [4] K. Hosokawa, H. Angerer, J. C. Puipe and N. Ibl, *Plating Surf. Finishing* **67** (1980) 52.
- [5] J. C. Puipe and N. Ibl, *Plating Surf. Finishing* **67** (1980) 68.
- [6] N. Ibl, *Surf. Techn.* **10** (1980) 81.
- [7] R. Olson, *Plating Surf. Finishing* **68** (1981) 38.
- [8] W. F. Fluemann, F. H. Reid, P. A. Mäusli and S. G. Steinemann, *ibid.* **67** (1980) 62.
- [9] D. S. Lashmore and J. F. Weinroth, *ibid.* **69** (1982) 72.
- [10] M. H. Gelchinski, L. Gal-Or and J. Yahalom, *J. Electrochem. Soc.* **129** (1982) 2677.
- [11] A. Knödler, C. Raub and E. Raub, *Metalloberfläche* **39** (1985) 21.
- [12] Y. Fukumoto, Y. Kawashima and T. Hayashi, *Surf. Coat. Technol.* **27** (1986) 145; *Plating Surf. Finishing* **73** (1986) 62.
- [13] D. S. Lashmore, I. Weisshaus and K. W. Pratt, *Plating Surf. Finishing* **73** (1986) 48.
- [14] M. Ratzker, D. S. Lashmore and K. W. Pratt, *ibid.* **73** (1986) 74.
- [15] M. D. Maksimovic and S. S. Djokic, *Surf. Coat. Technol.* **31** (1987) 325.
- [16] M. Cherkaoui, E. Chassaing and K. Vu Quang, *Plating Surf. Finishing* **74** (1987) 50; *Surf. Coat. Technol.* **34** (1988) 243.
- [17] C. C. Nee, W. Kim and R. Weil, *J. Electrochem. Soc.* **135** (1988) 1100.
- [18] J. Amblard, M. Froment and G. Maurin, *35th Mtg. Int. Soc. Electrochem.*, Berkeley CA, (1984), Ext. Abst. p.637.
- [19] J. Amblard, M. Froment, G. Maurin and N. Spyrellis, *170th Mtg. Electrochem. Soc.*, San Diego CA, (1986), Ext. Abstr. no. 469, p. 700.
- [20] J. Amblard, M. Froment and N. Spyrellis, *Surf. Techn.* **5** (1977) 205.
- [21] J. Amblard and M. Froment, *Faraday Disc. no. 12, Faraday Symp.* **12** (1978) 136, 201.
- [22] J. Amblard, I. Epelboin, M. Froment and G. Maurin, *J. Appl. Electrochem.* **9** (1979) 233.
- [23] J. Amblard, M. Froment, G. Maurin, N. Spyrellis and E. Trevisan-Souteyrand, *Electrochim. Acta* **28** (1983) 909.
- [24] *Idem*, *J. Microsc. Spectrosc. Electron* **6** (1981) 311.
- [25] N. Spyrellis, J. Amblard and G. Maurin, *Oberfläche-Surface* **26** (1985) 458.
- [26] N. Spyrellis, J. Amblard, M. Froment and G. Maurin, *J. Microsc. Spectrosc. Electron.* **12** (1987) 221.
- [27] G. Maurin and M. Froment, *Comptes Rendus Acad. Sci. Paris* **263C** (1966) 981.
- [28] *Idem*, *J. Microscopie* **7** (1968) 39.
- [29] G. Maurin, *Oberfläche-Surface* **11** (1970) 297, 309; **12** (1971) 8, 24, 47, 54.
- [30] J. Amblard, M. Froment and G. Maurin, *158th Symp. Electrocrystallization, Hollywood Florida* (1980) edited by R. Weil and R. G. Barradas, (The Electrochem. Soc., 1981) p. 179.
- [31] W. Paatsch, *Plating Surf. Finishing* **75** (1986) 52.
- [32] J. Amblard, M. Froment and S. Vitkova, *28th ISE Meeting*, Druzhba, Varna (1977) Ext. Abstr. no. 96, p. 427.
- [33] J. Amblard, G. Maurin, D. Mercier and N. Spyrellis, *Scripta Met.* **16** (1982) 579.
- [34] R. K. Dorsch, *J. Electroanal. Chem.* **21** (1969) 495.